CLIMATE CHANGE IN CHINA FROM 1880 TO 1998 AND ITS IMPACT ON THE ENVIRONMENTAL CONDITION

WEIHONG QIAN and YAFEN ZHU
Department of Atmospheric Sciences, Peking University, Beijing 100871, P.R. China
E-mail: qianwh@pku.edu.cn

Abstract. The global mean surface air temperature (SAT) or the Northern Hemisphere mean SAT has increased since the late nineteenth century, but the mean precipitation around the world has not formed a definite tendency to increase. A lot of studies showed that different climate and environmental changes during the past 100 years over various regions in the world were experienced. The climate change in China over the past 100 years and its impact on China's environmental conditions needs to be investigated in more detail.

Data sets of surface air temperature and atmospheric precipitation over China since 1880 up to the present are now available. In this paper, a drought index has been formulated corresponding to both the temperature and precipitation. Based on three series of temperature, precipitation, and drought index, interdecadal changes in all 7 regions of China and temperature differences among individual regions are analyzed. Some interesting facts are revealed using the wavelet transform method. In Northeast China, the aridification trend has become more serious since 1970s. Drought index in North China has also reached a high value during 1990s, which seems similar to that period 1920s–1940s. In Northwest China, the highest temperature appeared over the period 1930s–1940s. Along the Yangtze River valley in central eastern China and Southwest China, interdecadal high temperature occurred from 1920s to 1940s and in 1990s, but the drought climate mainly appeared from 1920s to early 1940s. In South China, temperature remained at a high value over the period 1910s–1940s, but the smaller-scale variation of drought index was remarkable from 1880 to 1998. Consequently, the quasi-20-year oscillation (smaller-scale variation) and the quasi-70-year oscillation (secular variation) obviously exist in temperature and precipitation series in different regions over China.

Climate change and intensified human activity in China have induced certain environmental evolutions, such as the frequency change of dust-storm event in northern China, no-flow in the lower reaches of the Yellow River and the runoff variation in Northwest China. On the other hand, frequent floods along the Yangtze River and high frequency of drought disaster have resulted in tremendous economic losses in the last decade in China. The primary reason for these happenings may be attributed to the evolution of the monsoon system in East Asian.

1. Introduction

Climate change and its impact on the environmental condition have attracted a great deal of interest for their theoretical and applied value (Berger and Labeyrie, 1987; Karl et al., 1995). Human activity, economic development as well as ecological evolution have been closely linked with the changes of climate and environment in the past centuries. Climate (temperature and precipitation) and environmental condition (drought and wetness) are the most direct factors, affecting agriculture

Climatic Change **50:** 419–444, 2001.

and the hydrological cycle. Global warming in the twentieth century has become a hot topic of climatology. The Intergovernment Panel on Climate Change (IPCC) report of 1995 indicated that human-induced 'greenhouse' warming affects have made global mean surface air temperature (SAT) rise about 0.3 $\sim$ 0.6 degree in the recent 100 years (IPCC, 1996). A fact has been identified that two warming periods appeared respectively in 1920s $\sim$1940s and from 1970s till now (Diaz and Quayle, 1980; Jones et al., 1986a; Diaz, 1986; Yamamoto et al., 1986; Trenberth, 1990; Miller et al., 1994; Fu et al., 1999).

In the twentieth century, population increases and economic prosperity in China were mainly concentrated in Northeast China, the Yellow River valley, the Yangtze River valley and South China. Climate change of the twentieth century and its impact on the environmental condition in China needs to be investigated in more details.

Data sets of surface air temperature and atmospheric precipitation for more than 100 years since 1880 over China are now available. The data source and constructed drought index are described in the following sections. Interdecadal changes of the temperature, precipitation and drought indices in Northeast China, North China, Northwest China, East China, Central China, Southwest China, and South China are analyzed in Sections 3, 4 and 5, respectively. Regional differences of temperature are compared in Section 6. Signal analysis for temperature and precipitation in all 7 regions by the method of wavelet transform is made in Section 7. A discussion concerning the consequence of climate change in different regions over China is given in Section 8. The change of monsoon circulation over East Asia is described in Section 9. Finally, the conclusion is presented in Section 10.

2. Data Source

Data sets used in the present study are the annual mean surface air temperature anomalies (SATA) of 10 regions and the four seasonal (Jan.–Feb.–March; April–May–June; July–Aug.–Sep.; Oct.–Nov.–Dec.) precipitation of 35 stations over China from 1880 to 1998 (Wang et al., 1998; Ye et al., 1998). Several data sources have been used in the construction. Such sources include ice core (Yao et al., 1995) in western China (Guliya and Dunde in the western and north Tibet Plateau), 5-grade data of temperature and precipitation based on the documented records mainly in eastern China, long-term observations notably in Shanghai since 1841 and Beijing after 1873. All stations providing data source are displayed in Figure 1 with 10 regions divided by Wang et al. (1998), including Taiwan, Tibet and far northwest provinces, but only the data set over 7 regions is used in this paper. From south to north, the studied area covering the large part of the East Asian monsoon region and their numbers are listed. Region 1 refers to South China or the Xijiang River valley. Regions 2, 3 and 4 are located in Southwest China, Central China and East China along the Yangtze River valley. Regions 5 and 6 are

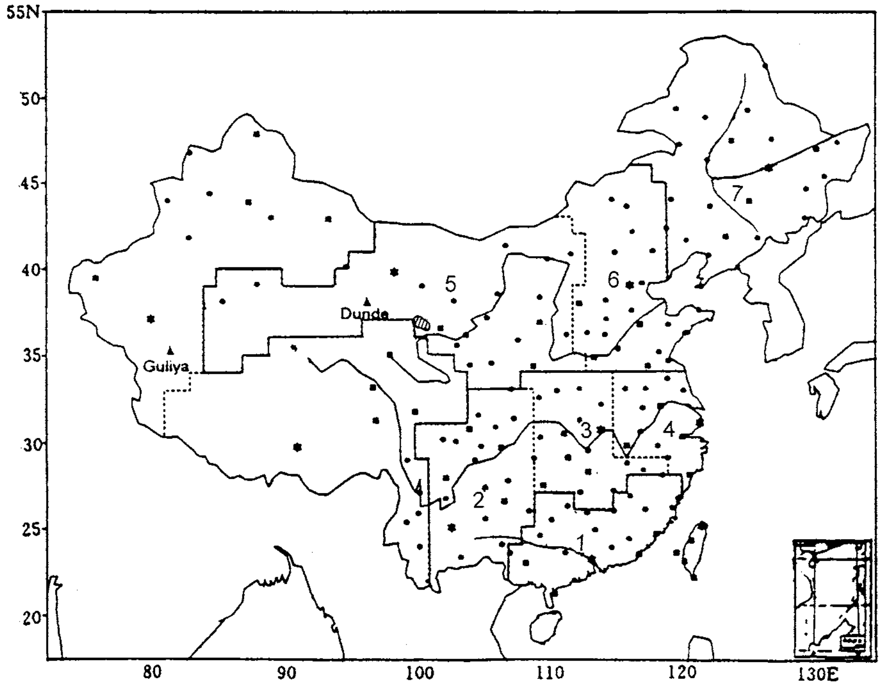

Figure 1. All stations of data source displayed by Wang et al. (1998) in China. ▲ indicates the locations of ice-core sampling; ● the observed and grade stations for surface air temperature and precipitation; ■ representative stations obtained proxy data from the place; ★ central stations in every region. Dashed line divided 10 regions and solid line the boundary of different valleys. Separated regions in China: 1. South China, 2. Southwest China, 3. Central China, 4. East China, 5. Northwest China, 6. North China and 7. Northeast China. Four river valleys from south to north in eastern China include the Xijiang River in Region 1, the Yangtze River valley covering the Regions 2, 3 and 4, the Yellow River valley in the Regions 5 and 6, and the Songhuajiang river valley in Region 7.

Northwest China and North China along the Yellow River valley. Finally, Region 7 is Northeast China or the Songhuajiang River valley. SATA series at each region were calculated relative to the mean of 30 years between 1961 and 1990 and relative to the average-area of all stations in that region. All 35 stations for precipitation series are also located in these 7 regions. Precipitation series at each region were constructed using the mean of precipitation of all stations in that region. Basically, the climate change of four valleys from south to north will receive special attention in this paper.

Having constructed the data series of SATA and precipitation in all 7 regions, a drought index is formulated in the present study. Thus, three data series, including SATA (T), precipitation (R) and drought index (DI) will be examined in different regions for different periods.

3. Temperature Change

In the past 100 years, the rapid change of SAT in the Northern Hemisphere is characterized by a sudden rise in temperature around 1920 (Fu et al., 1999; Jones et al., 1986b). Using the SAT data from 196 Chinese stations for 1951–1995, Zhai et al. (1999) found that the mean minimum temperature increased significantly throughout China, particularly at the higher latitudes during the past 40 years. However, the secular changes of SAT for different periods and regions in China as well as their contributions to global warming are unknown completely.

Figure 2 shows the SATA in Northeast China, North China, Northwest China, East China, Central China, Southwest China, South China and total mean of 7 regions, respectively. The SATA time series is displayed by light solid-line, while the heavy solid-line indicates the 7-point running mean to the series. The smooth curve, which filtered out the smaller-scale variations and represents the secular variations, is the 10-order polynomial fit to the original series. The dashed lines crossing different time series connect most maximum or minimum of the smooth curves. In China for the total 7-region, the historical highest record was observed in 1998 since 1880. A long warm period is found from 1920s to 1940s, which was advanced by about 10 years related to that warming of the Northern Hemisphere (NH). The second warming started from late 1980s, which was delayed by about 10 years relative to the NH SATA series. Two similar cold periods in strength are found over the periods 1880s $\sim$ 1900s and 1960s $\sim$ 1970s for the total 7-region. It should be noted that the second cold period in the series of the NH SATA was relatively warmer than the first one (see the series of Jones, 1986b).

From the series of SATA in Northeast (NE) China, secular change shows that the coolest period appeared in 1900s $\sim$ 1910s with the mean SATA about –0.9 °C. During the period between 1920s and mid 1970s, the temperature in NE China maintained a relatively stable level, so a temperature increase by 0.7 °C was found during the 1910s. From 1970s to the end of the twentieth century, the temperature in NE China rose about 1 °C. Totally, the temperature has increased by about 2 °C from late 1900s to late 1990s for the secular change. The change of SAT was in phase with that of the NH, but the amplitude was larger, so SAT rising must have a positive contribution to the change of the NH temperature and to the global warming. The lowest SATA was found in 1908 (–2.0 °C) while the highest one in 1998 with their relative difference of 4 °C.

In North China, two periods with low-temperature appeared before mid 1910s and between 1950s and 1960s. The first period of high temperature was in 1920s $\sim$ 1940s while the second one starts from 1980s. The largest temperature difference around 1.5 °C can be found between mid 1950s and late 1990s from the running mean curve. This pattern of SAT change in North China is drastically different from that in NE China.

The period with the highest SAT in Northwest (NW) China can be clearly seen from late 1930s to 1940s. Two relatively cold periods are found during 1890s $\sim$

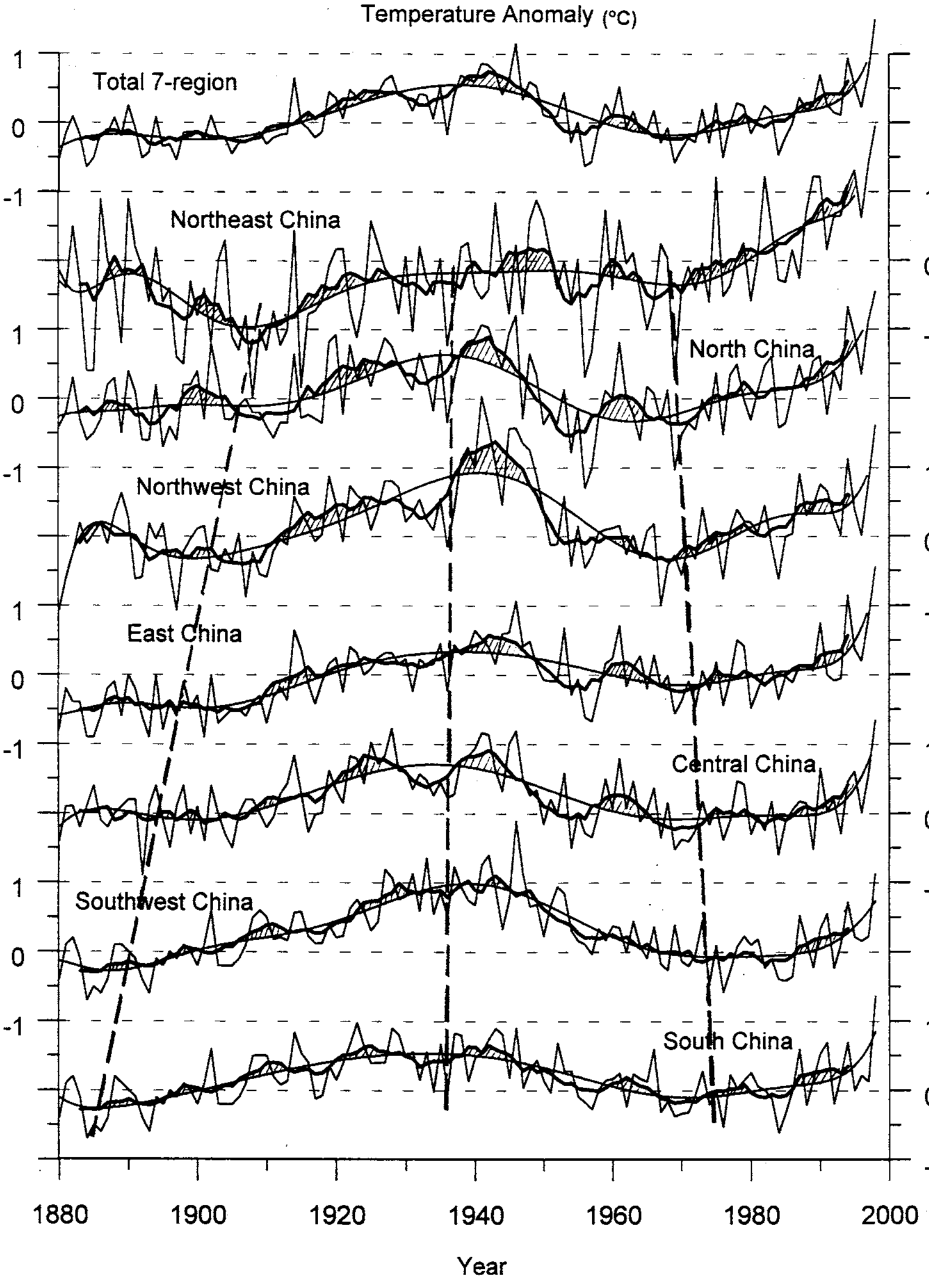

Figure 2. Time series (light solid line) of temperature anomalies (°C) from 1880 to 1998 in different regions over China and total 7-region mean. Smooth curve and heavy solid line are the 10-order polynomial fit and the 7-point running mean to the series. The dashed lines crossing different time series connect most maximum or minimum of the smooth curves. The shaded areas indicate the differences between running mean and smooth curve.

1900s and 1960s $\sim$ mid 1970s. Since the 1980s, the temperature has gradually increased, but the SAT did not exceed the averaged value of SAT in 1940s.

In East China, the first period of relative high temperature occurred during the 1920s $\sim$ 1940s while the second one beginning from the 1990s. Large temperature difference can be found over the period 1900s $\sim$ 1920s. In Central China, the first cooling is particularly weaker than that in East China, but the first warming is stronger than the latter. Along the Yangtze River valley, the largest amplitude of SAT change is found in Southwest China if comparing it with SATA changes in East China and Central China. The change of SAT in South China is small in amplitude relative to other regions in China.

Two implications can be given from the SAT changes in Figure 2. Firstly, SAT has a secular change in all 7 regions. The first warm period commonly occurred over the 1920s $\sim$ 1940s, while the second one started from the late 1970s in northern China (i.e., regions 5, 6, 7) and from the late 1980s in southern China (i.e., regions 1, 2, 3, 4). The first cold period in South China was earlier than that in Northeast China by about 10–20 years, while the second cold period in Northeast China was earlier than that in South China by about 10 years. Secondly, smaller-scale variations of SATA can be found in Figure 2 with shaded areas. Positive departures, such as in the 1940s, and negative ones in the 1930s and 1950s characterized these smaller-scale variations in different regions.

4. Precipitation Change

Precipitation changes in all the 7 regions over China are shown in Figure 3. The light solid line indicates the annual precipitation totals, the heavy solid-line denotes the 7-point running mean to precipitation series. Many smaller-scale variations can be found in all series. To compare with the secular variation of SATA, the smooth curve still applied the 10-order polynomial to the original series. Totally in China, annual mean precipitation is about 1000 mm. It could be seen from Figure 3 that, not only in the individual regions but also in all the 7 regions, the precipitation changes are more complex than the SATA. Through the following description and signal analysis for each series, it may be found that the smooth curve of 10-order polynomial reflects some internal information with secular variation contained in the original series.

In Northeast China, the periods of below normal precipitation could be found over the 1900s $\sim$ 1930s and after the late 1960s, while the periods of more precipitation over the 1880s $\sim$ 1890s and from 1940s to early 1960s by the smooth curve. Shaded areas denote six smaller-scale variations related to the smooth curve. Annual mean precipitation in North China was slightly more than that in Northeast China. The secular change of precipitation in North China was similar to that in Northeast China. Recent study shows that the quasi-20-year oscillation existed in the variation of precipitation over North China (Yan, 1999). In Northwest

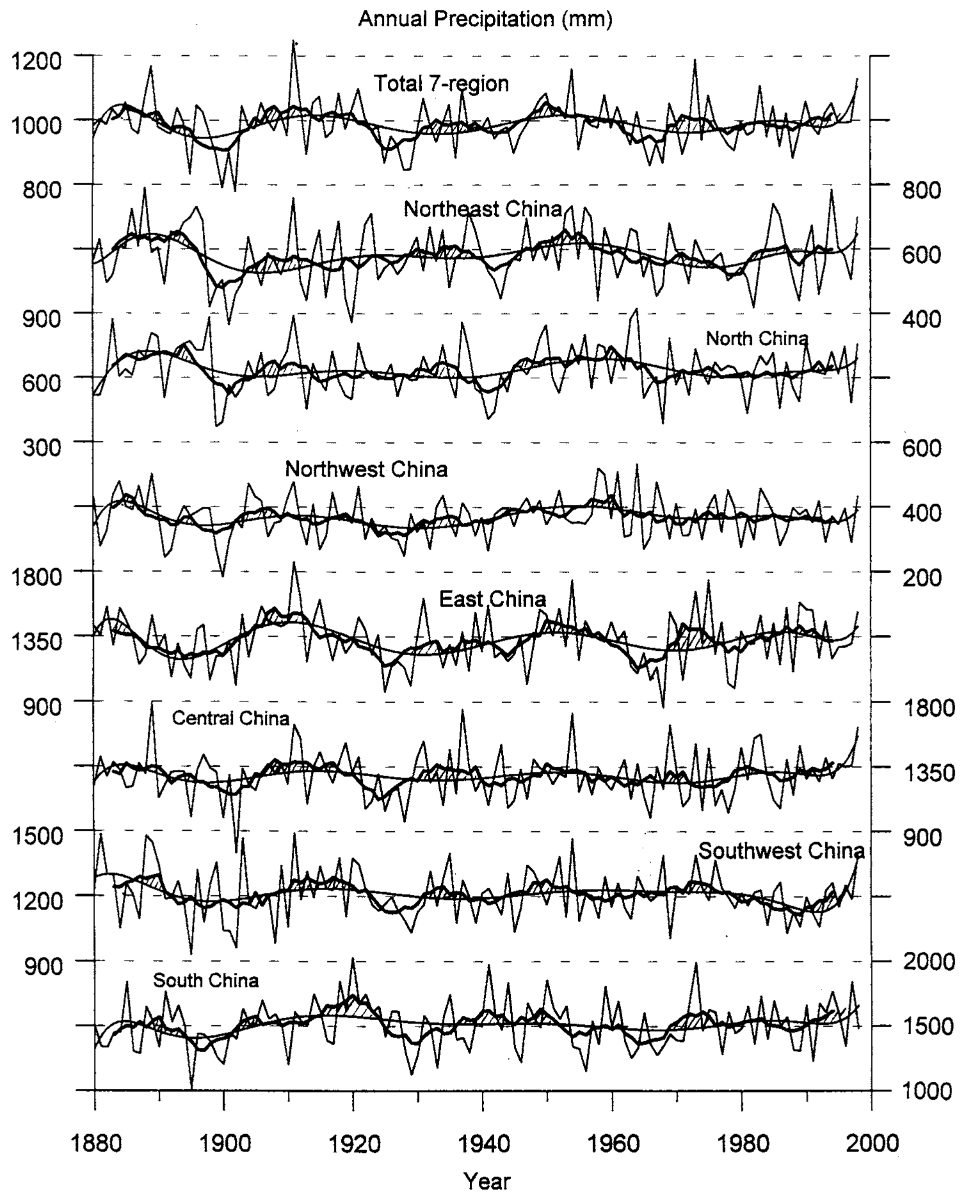

Figure 3. Same as in Figure 2 but for the time series of annual precipitation (mm).

China, annual mean precipitation is slightly less than 400 mm and relatively more precipitation appeared from 1940s to 1960s except for the short period in 1880s.

In East China, precipitation over the 1900s $\sim$ 1910s and after the 1980s for the secular change had positive anomalies related to the level of 1350 mm. The smaller-scale variations of precipitation are also predominant in East China with about 6 processes related to the smooth curve. Similar precipitation mean as well as the secular change and smaller-scale variations are found in Central China. In Southwest China, annual mean of precipitation was about 1200 mm. The relatively less precipitation in Southwest China occurred in late 1890s ∼ early 1900s and in 1980s. In South China, the precipitation mean around 1500 mm is the highest one, compared with that in other regions.

Unlike the SATA series in all 7 regions, secular change and smaller-scale variation of precipitation had various phases in different regions. Their phase relations will be identified by the analysis of wavelet transform.

5. Drought Index and its Change

As is well known, China is strongly influenced by the East Asian monsoon. During the winter the weather is always cold and dry, while in summer the rainbelt moves gradually from the south to the north. Both dryness and wetness have such direct impact on the abundance or deficiency of agricultural productions in China that drought and flood are the major climate disasters concerning both the Chinese government and the general public. To present the impact of temperature and precipitation anomalies on agriculture and life-supporting environment, a drought index is defined and formulated. An index defined by Pedj (1975) has been widely used in Russia in the past two decades for documenting droughts and moisture surplus conditions. It represents the difference between standardized anomalies of surface air temperature and atmospheric precipitation over the area of interest. Recently, Gruza et al. (1999) applied this index to study the climate change during the twentieth century for the Russian Federation. In this paper, a drought index is defined by

$$DI = \Delta T/S_T - \Delta P/S_P \,,$$

where, DI is the drought index; ΔT and ΔP are the anomalies of surface air temperature and precipitation relative to the mean between 1880 and 1998; S_T and S_P are the standard deviations of temperature and precipitation. The standard deviations in different regions are listed in Table I. From Table I, it is noted that the standard deviations of temperature and precipitation in all the 7 regions are 0.40 °C and 81.60 mm respectively. For the individual regions, the largest deviation of temperature is found in Northeast China with 0.74 °C while the lowest in South China with 0.39 °C. Opposite situation is noted from the deviation of precipitation with the largest one in South China (194.18 mm) and lowest in North China (75.24 mm). The relatively lower deviation of precipitation also exists in the middle reaches (Central China) of the Yangtze River, compared to other areas along the river. This index indicates that the higher surface air temperature and the less precipitation will result in drier climate in the defined region.

Figure 4 shows the drought indices in different regions over China. For all 7 regions as a whole, the major drought period appeared over the 1920s ∼ 1940s.

Table I
The standard deviations of surface air temperature and precipitation in different regions over China

Region	S_T (°C)	S_P (mm)
Total 7-region	0.40	81.60
Northeast China	0.74	84.48
North China	0.54	75.24
Northwest China	0.58	161.09
East China	0.45	184.23
Central China	0.44	109.67
Southwest China	0.49	128.98
South China	0.39	194.18

Since the 1980s, the recent drought period started in China, but it does not exceed the previous drought. However, the drought evolutions were various in different regions over China from 1880 to 1998. Noting the region of Northeast China, the aridification trend has become more serious since 1970s. The situation in North China is different from that in Northeast China. The first dry period with the secular change in North China appeared between 1920s and 1940s while the second one mainly in 1990s. The drought level in the late 1990s has reached that of the first one. In Northwest China, drought was remarkable over the period 1920s $\sim$ 1940s, particularly during the 1940s. From late 1970s to early 1990s, drought happened again in Northwest China, but it has not exceeded the level in 1940s. During the past 100 years, the fluctuations of drought in both secular timescale and smaller timescale are rather obvious in East China. In Central China and Southwest China, the major drought periods are basically the same as those in East China. In South China the amplitude of secular variations is the smallest compared to other regions. Generally, drought in China mainly appeared in 1920s $\sim$ 1940s except in Northeast China and South China. The trend of drought development in Northeast China and North China over the lower reaches of the Yellow River needs special attention in the coming decade.

6. Regional Difference of Temperature

A comparison of temperature difference (TD) related to different regions is made in Figure 5. The TD time series is displayed by light solid line and the smooth curve is the 10-order polynomial fit to the original series, while the heavy solid line indicates the 7-point running mean to the TD series. The TD time series between Northeast China and North China is shown in the first upper panel. Before 1940s,

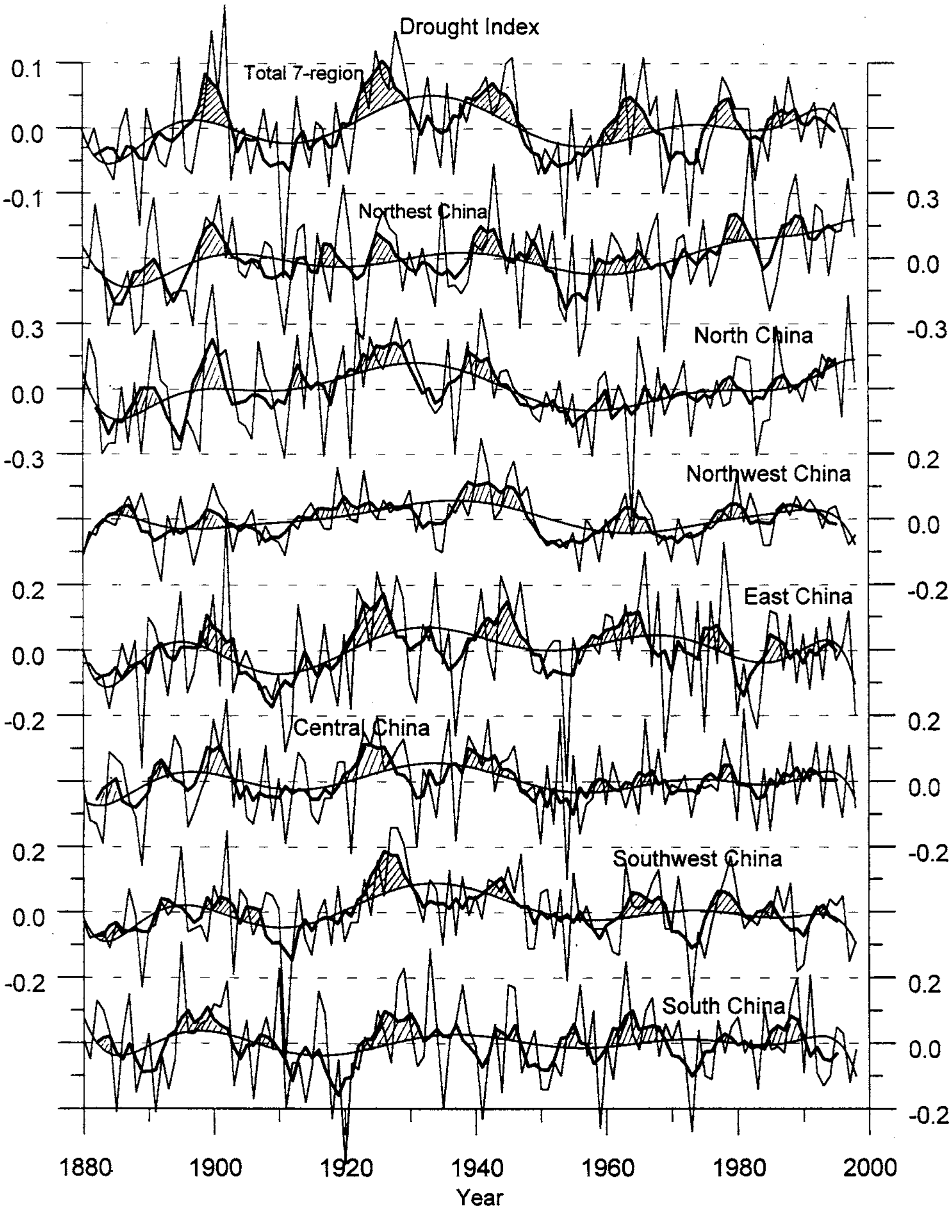

Figure 4. Same as in Figure 2 but for the time series of drought index.

the TD is negative, i.e., the SATA was higher in North China than that in Northeast China. However, the situation abruptly changed in late 1940s. Since 1980s, the SATA in Northeast China has become higher than that in North China. The sudden change of temperature contrast between these two regions in 1940s needs further investigation.

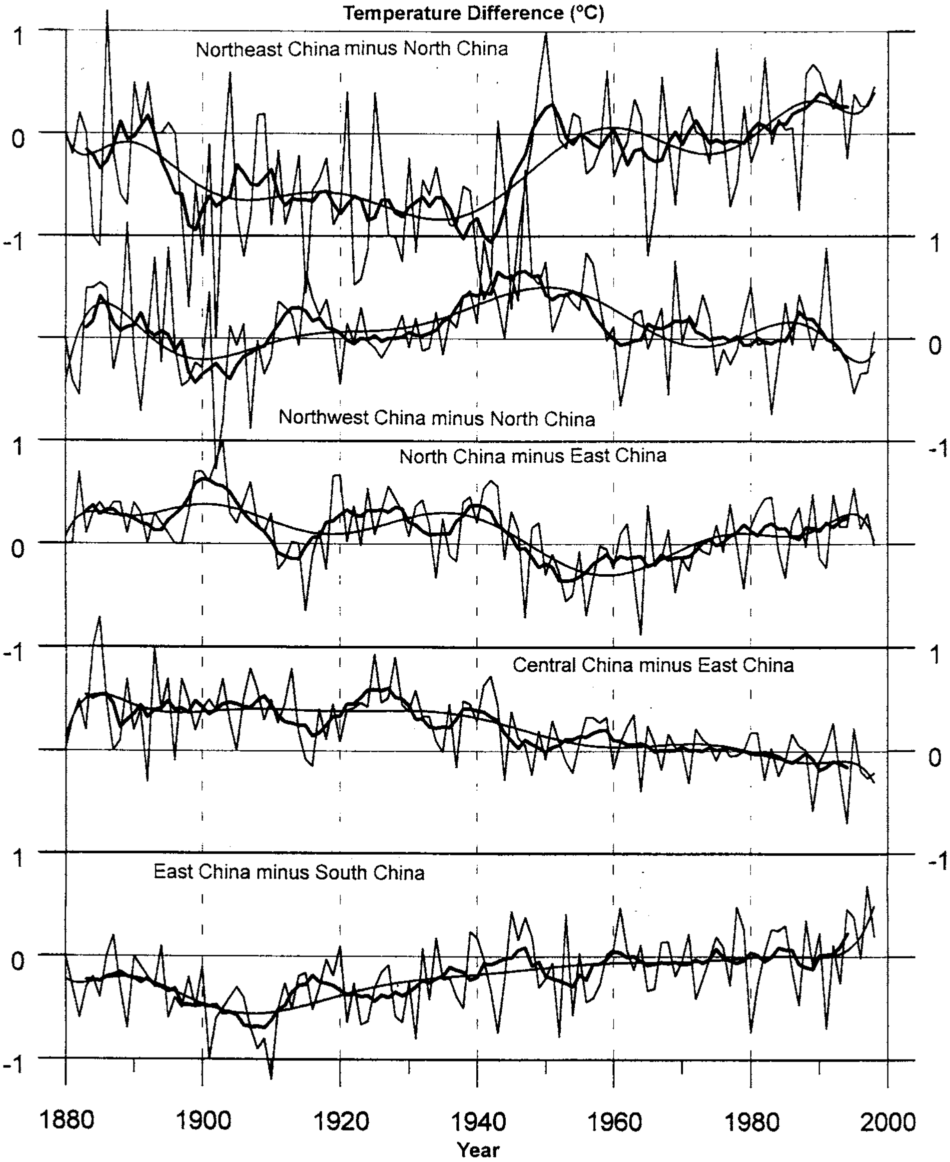

Figure 5. The difference series (°C) of SATA between different regions. Smooth curve and heavy solid line are the 10-order polynomial fit and the 7-point running mean to the series.

Along the Yellow River valley, the changes of SATA in Northwest China and North China are shown in the second panel of Figure 5. Positive SATA was more predominant in Northwest China than that in North China during late 1930s ~ 1950s. After the 1960s, the difference of SATA along the Yellow River valley became smaller. The SAT in North China was lower than that in East China during

1950s $\sim$ 1960s, but the situation was reversed from 1880s to early 1940s and since the mid-1970s. Along the Yangtze River in the mid-low reaches, the difference of SATA between Central China and East China gradually decreased from a positive value to a negative one. After the 1980s, the positive SATA in East China became larger than that in Central China. It implies that the climate in East China has become warmer than that in Central China during the last two decades. The opposite trend of SATA contrast between East China and South China can be found in the final panel of Figure 5, which means that the climate in East China also became warmer than that in South China in the end of the last century. During the late nineteenth century and the first half of the twentieth century, the temperature contrast between South China and East China was rather larger than that in recent decades.

Figure 6 shows the differences of SATA among the Songhuajiang River valley in Northeast China, the Yellow River valley in North China and Northwest China, the Yangtze River valley in East China, Central China and Southwest China, and the Xijiang River valley in South China. The differences of SATA between Northeast China and other valleys are displayed in the first three panels of Figure 6. Evidently, the SAT in Northeast China was rather low before the 1960s, particularly between 1900s and 1940s, compared with those in other three valleys. Since the 1980s, the speed of SAT rising in Northeast China has exceeded that in other three valleys.

SATA differences in the Yellow River valley related to the Yangtze River valley and South China exhibit several fluctuations from 1880 to 1998. Lower temperature in the Yellow River valley related to the Yangtze River valley and South China was located in the 1900s $\sim$ early 1910s and the 1950s $\sim$ 1960s. During the late 1930s $\sim$ 1940s, a positive difference appeared. Another positive difference starting from the 1980s implies that warming in the Yellow River valley was stronger than that in the Yangtze River valley and South China. Between the Yangtze River valley and South China, SATA difference was the smallest compared with those in other regions from 1880 to 1998. Particularly after the 1960s, the difference was nearly zero, i.e., the trend of SAT change was consistent in the Yangtze River valley and South China.

7. Signal Analysis

As regards the descriptions in Sections 3 and 4, some major oscillation signals are found in the time series of SATA and precipitation. The wavelet transform method (Lau and Weng, 1995; Jiang et al., 1997) can extract the major information from the original series (SATA and precipitation) in different regions. In this study, the mother function of 'Mexican hat' has been adopted to analyze each of all the series. The wavelet coefficients $W(a, b)$ with positive-negative anomalies in this study present the high-low temperature variations or the more-less precipitation variations on various timescales (a) and at different time points (b: year). $W(a, b) > 0$

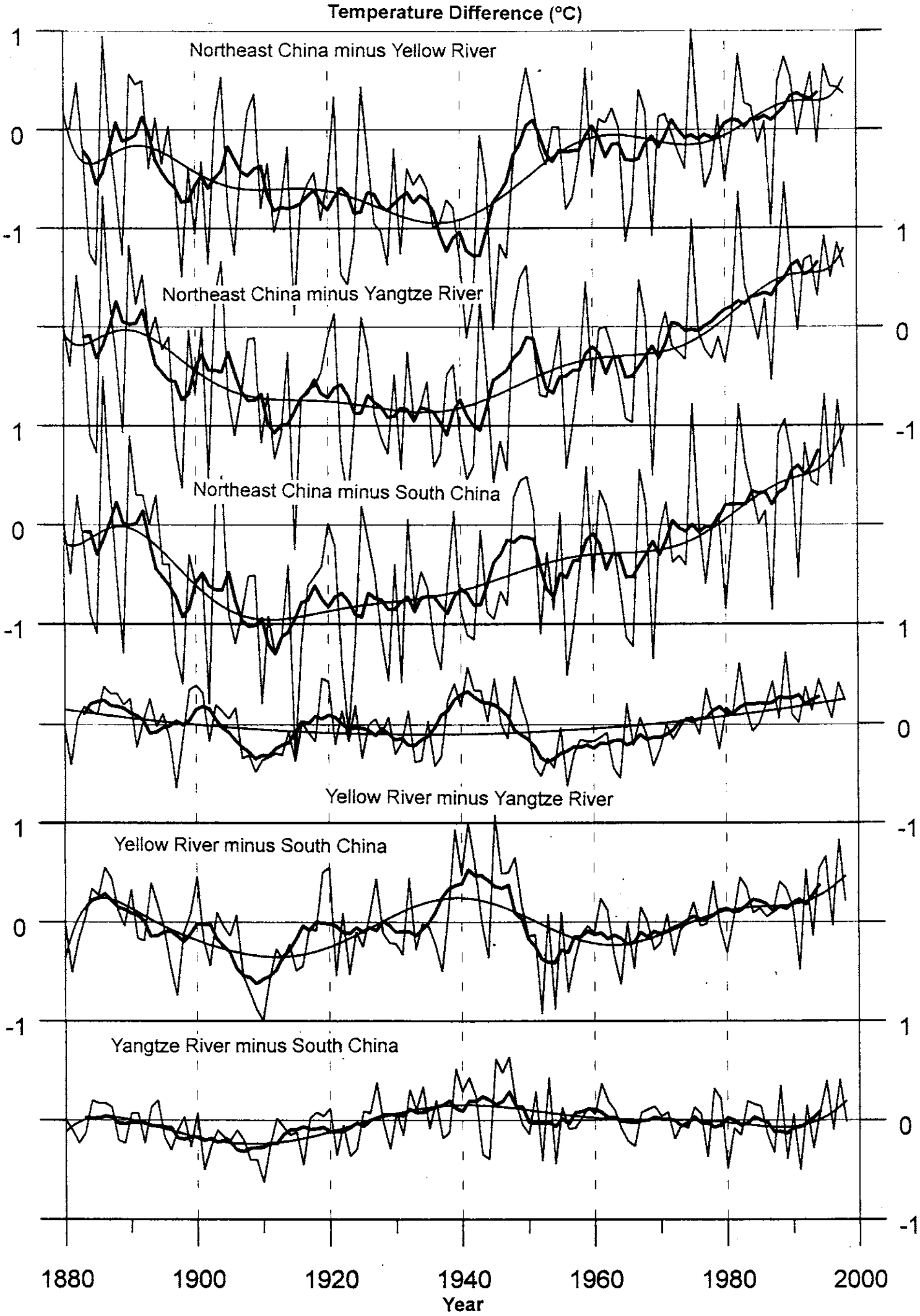

Figure 6. Same as in Figure 5 but for the difference series (°C) of SATA between different valleys.

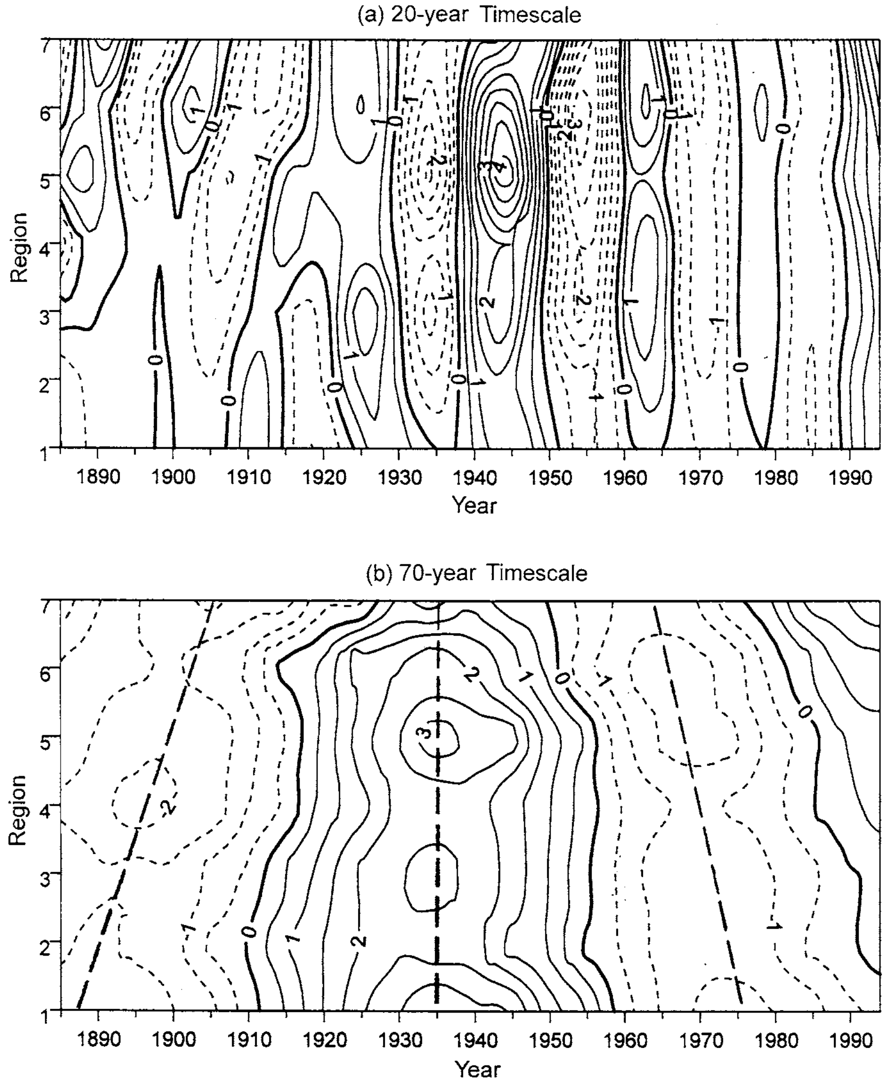

Figure 7. Wavelet coefficients of SATA time series in all 7 regions at timescales of (a) 20 years and (b) 70 years from 1885 to 1995. Regions from 1 to 7 cross the four valleys, mostly from south to north in China.

responds to the high temperature or more precipitation, and $W(a, b) < 0$ to the reversed situations. Having made wavelet transform, two prominent signals (regular variation and large amplitude) with 20-year and 70-year timescales can be obtained from the temperature and precipitation series.

Figure 7 shows the components of wavelet coefficients of SATA with two timescales of 20 years and 70 years for the 7 regions. From Figure 7a, regular transitions of cold (negative coefficient) and warm (positive coefficient) with the mean spell about 10 years can be found since 1930 in all 7 regions. This result indicates that cold surge (relatively lower temperature) or heat wave (high temperature) can hit the whole China simultaneously, but the large-amplitude fluctuation appeared in northern China related to the small one in southern China. On this timescale, the highest temperature appeared in Northwest China during 1940s while the second one late in the 1990s in Northeast China. According to Figure 2, the highest temperature in the last century was found in 1998. The distributions of wavelet coefficients at the 20-year timescale shown in Figure 7a are mostly the reflection of shaded areas in Figure 2. In this timescale, there are 6–7-pair transitions over the period from 1880s to 1990s so that the quasi-20-year oscillations are manifested in the temperature series.

At the 70-year timescale, cold/warm oscillations shown in Figure 7b indicates that the positive or negative departures can also influence the whole China, but the large departures are found in northern China. The second warming spell in NE China is the earliest since late 1970s with the largest departure late in the 1990s. With this timescale, a warming spell has just started in China. From Figure 7b, the first negative maximum (left dashed line) appeared from southern China around the 1880s to northern China in the 1900s. The positive maximum (middle dashed line) occurred in the 1930s in all 7 regions. The second negative maximum (right dashed line) is found from northern China in the 1960s to southern China in the late 1970s. This situation is the reflection of dashed lines shown in Figure 2. Consequently, the quasi-70-year oscillation can be noted in these temperature variations.

The wavelet coefficients of annual precipitation for the 7 regions with the timescales of 20 years and 70 years are displayed in Figures 8a,b. During some decades, floods appeared in the whole China from south to north, such as those in 1880s, late 1900s–early 1910s, 1930s, 1950s, 1970s (Figure 8a). And during some other decades, floods only took place in parts of China. Usually, three obvious variance centers of precipitation are located in Southwest China, East China and North China, but the departure in North China is smaller. The shaded areas in Figure 3 can also be identified from Figure 8a with the positive and negative coefficient centers.

Shown in Figure 8b, positive/negative wavelet coefficients indicate the secular oscillation of annual precipitation for all the 7 regions in China. A phenomenon must be noted that positive and negative distributions of precipitation anomalies are opposite in southern and northern China. Before the 1900s, positive anomaly of precipitation appeared in northern China while the negative in the Yangtze River and South China. Over the 1910s to 1930s, less precipitation occurred in northern China and the lower Yangtze River while more rainfall occurred in the upper Yangtze River. The situation between 1950s and 1960s was reversed with more precipitation in northern China and less along the Yangtze River. Since the late 1980s, above normal rainfall has appeared along the Yangtze River while the dry air persists in northern China. Although there is a difference in the phases for these coefficients, the quasi-70-year oscillation exists in these time series.

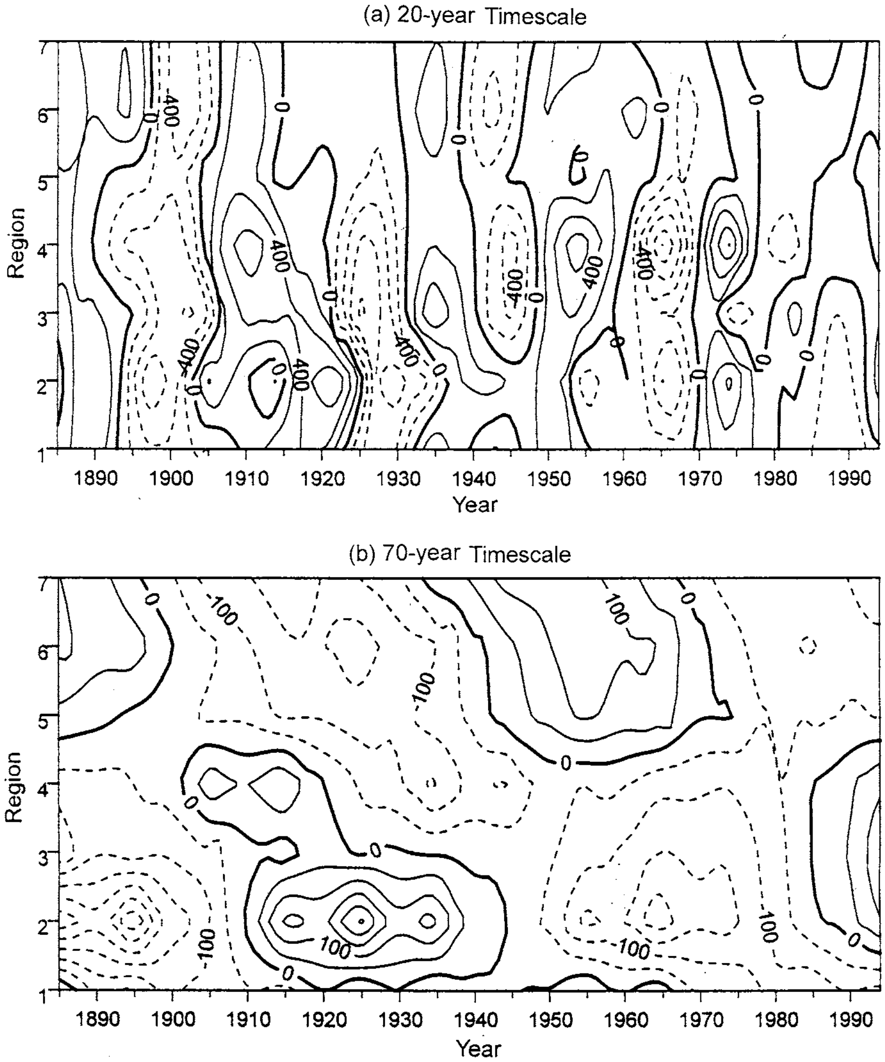

Figure 8. Same as in Figure 7 but for the annual precipitation in all 7 regions.

Comparing Figure 7 with Figure 8, an important fact can be inferred that the central locations of temperature and precipitation variations are different in China. For the temperature, the relatively large variation is located in the Yellow River, particularly in Northwest China. For the precipitation, the large variation is situated along the Yangtze River, mainly in Southwest China and East China. Another fact implies the two major components with the 20-year and 70-year oscillations are orthogonal. Namely, the 10-order polynomial and 7-year running average operating to the temperature and precipitation series imply that two natural oscillations exist within the climate system over East Asia.

8. Consequence of Climate Change

With the investigation given above, some basic characteristics of climate change have been described and some major signals have also been extracted from the original series of temperature and precipitation in China. According to these analyses, certain environmental changes related to major variations of climatic parameters will be discussed as follows.

8.1. MAJOR DROUGHT DISASTER IN CHINA

According to the report of the damage in China (1949–1995), among all disasters the drought disaster causes the largest economic loss (Damage Report, 1995). From 1949 to 1995, altogether 12 years of major drought disaster (covered at least one valley) have happened in China, all of which were mainly concentrated in the three periods of 1959–1961, 1978–1982 and 1986–1994, that also found within the drought spells (Figure 4). For the period of 1986–1994, the years of 6 major drought disasters appeared. This result shows that the frequency of drought disaster has greatly increased in the recent decade.

To see the drought disasters in different regions over eastern China, Figure 9 gives the area ratios affected by drought and the area ratios experiencing drought disaster from 1949 to 1990, according to the series of Zhang et al. (1997). In Northeast China, the ratios show a trend of increase since the 1970s, which is consistent with the variations of DI, particularly for the years of 1982 and 1989. In North China and Northwest China, the periods of high DI in Figure 4 and the concentrated periods of drought disaster show consistency. In East China, three disaster periods around 1960, 1978 and 1988 are consistent with those DI, shown in Figure 4. In Southwest China, disasters mainly appeared in 1960s and 1980s. The consistent relationship between drought disaster and positive DI can also be seen from Figure 9 and 4 in South China but the ratios are the lowest compared with that in other regions. It is noted that the drought disaster mainly appeared in northern China, particularly in Northeast China.

8.2. DISASTER AND BENEFIT IN NORTHEAST CHINA

From Figures 7b and 8b, an important feature of climatic change in Northeast China is temperature rising, precipitation reducing and drought strengthening, which finally resulted in evaporation increasing in the last two decades. Excessive evaporation upsets the normal hydrological cycle through precipitation and runoff. Thus, soil salinization, particularly in the western part of Northeast China has become a major obstacle for the sustained development of agriculture.

Besides the negative effects of temperature rising, the summer plants such as bean, rice and mealie can obtain enough light and heat for their harvest in the past two decades. This situation is greatly different from that 20 years ago when the summer low-temperature was a major disaster for agriculture in Northeast China

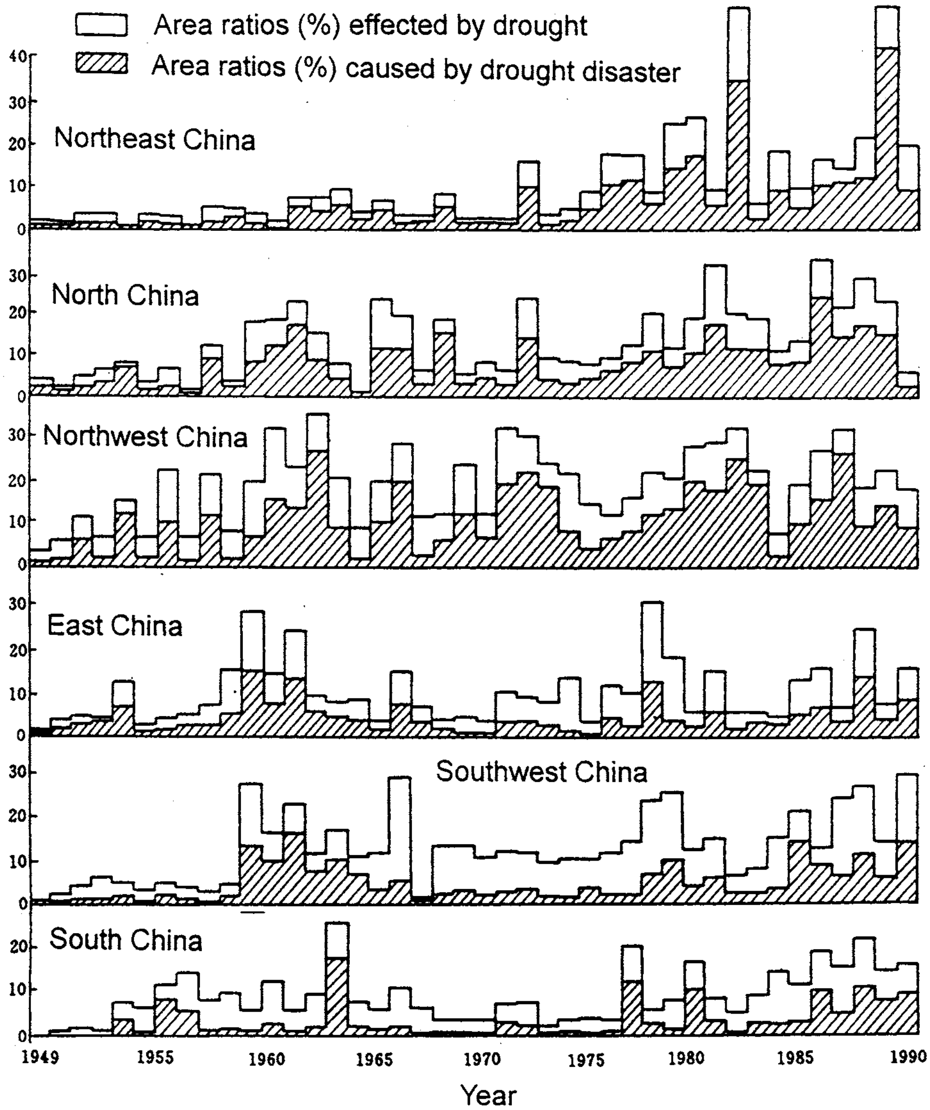

Figure 9. The area ratios (%) effected by drought and the area ratios (%) experiencing drought disaster from 1949 to 1990 in different regions related to the total area in each region.

(Wang and Zhao, 1987). From 1949 to 1981, low-temperature disaster appeared in Northeast China 19 times, but for the period 1982–1995 only appeared 4 times (Damage Report, 1995).

8.3. RUNOFF VARIATION IN THE UPPER YELLOW RIVER

Water resource of the Yellow River mainly comes from Northwest China and the northeastern Tibet Plateau, i.e., from the upper reaches of the Yellow River valley.

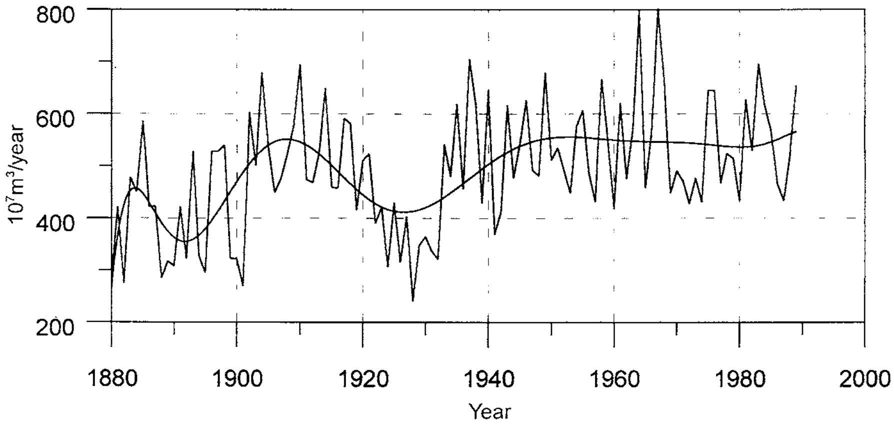

Figure 10. Annual runoff series (10^7 m^3/year) from Sanmenxia gauge station at the upper reach of the Yellow River for 1880 ∼ 1989. The smooth curve is the 10-order polynomial fit to the series.

Figure 10 is the annual runoff from 1880 to 1989 for Sanmenxia gauge station at the upper reach of the Yellow River, based on the series of Wang et al. (1999). From Figure 10, it can be noted that two periods of lower runoff mainly appeared over the 1890s and from 1920s to early 1930s. From 1940s to 1960s, there was a period of relatively higher runoff. The secular variations of runoff in Figure 10 and the annual precipitation in Northwest China with the smooth curve show the consistent relation in their phase. Some interannual variations, such as for the low runoff in 1890, 1900 and 1928, can also be explained by the annual precipitation in Northwest China. These relations indicate that the runoff in the upper reaches of the Yellow River depends mainly on the regional precipitation.

8.4. DUST STORM IN NORTH CHINA

The winter of 1999–2000 year was a very cold period related to the last decade, then 9 dust storms were observed at Beijing weather station in spring of 2000. According to the definition by Goudie and Middleton (1999), the dust event caused by aeolian processes includes four types: dust storms, dust haze, blowing dust and dust whirls. In this paper, only the first three types are considered in Beijing, China. The annual dust days can be seen from Figure 11, based on the observation of spring (the main dust-storm season, Mar–Apr–May) from Beijing weather station for 1950 ∼ 1999. The annual days show a trend of decrease in the last 50 years. In the early 1960s and in the 1990s, less annual days are observed. This is consistent with the high temperature in North China while the more annual days near 1955 and from 1965 to 1970s are due to the lower temperatures here. In Northern China the precipitation mainly falls in summer from June to September while the annual temperature depends mostly on whether cold air is active and strong in the winter-spring period. This evidence has been described by Zhang (1984) using his-

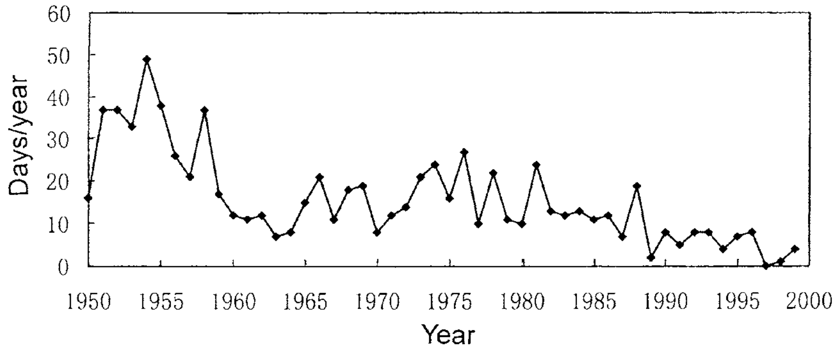

Figure 11. Annual dust days from 1950 to 1999 in Beijing, China.

torical document records in China for about 1700 years that the dust-fall frequently happened under the background of dry-cold climate.

8.5. NO-FLOW IN THE YELLOW RIVER

From 1970s to late 1990s, the annual spell of no-flow in the lower reaches of the Yellow River is becoming longer year to year. Table II lists some statistics of no-flow near the Li-jin gauge station in the lower reach of the Yellow River, according to the data of Yao et al. (1999). From 1972 to 1997, altogether 20 years of no-flow happened and four exceptions appeared in 1973, 1977, 1984 $\sim$ 1986 and 1990. These years of exceptions with yearly flow along the whole river were consistent with the years of more rainfall or low drought index in the river. The times of yearly no-flow and length of yearly no-flow are directly proportioned to the days of no-flow. In 1981, 36 no-flow days, 5 no-flow times and 662 km no-flow length were recorded, which coincided with less precipitation along the Yellow River in that year (Figure 3). Another year, 1997, with the highest record of no-flow days (226 days), no-flow times (13) and no-flow length (700 km) met less precipitation and high DI in North China. The no-flow in recent decades has become more sensitive to rainfall and DI than before 1970, which may be attributed to the increase of human activity and climatic change along the river. As seen from Figures 8b and 4, precipitation along the Yellow River had a decreasing trend since late 1970s and the drought index has greatly increased particularly during the 1990s in North China. Obviously, the drought index is a synthesized environmental indicator, which can well represent the secular trend of no-flow in the Yellow River.

8.6. FLOODS ALONG THE YANGTZE RIVER

Flood is caused by heavy rainfall. A significant consequence of climatic change along the Yangtze River is frequent floods since mid 1980s due to the increment of rainfall strength, which can be seen clearly from Figure 8b. Historically, the major floods in 1954 and 1975 over East China (Damage Report, 1995) were

Table II

Statistics of no-flow at the Li-jin gauge station in the lower reach of the Yellow River

Year	No-flow days	No-flow times	No-flow length (km)
1972	19	3	310
1974	20	2	316
1975	13	2	278
1976	8	1	166
1978	5	4	104
1979	21	2	278
1980	8	3	104
1981	36	5	662
1982	10	1	278
1983	5	1	104
1987	17	2	216
1988	5	2	150
1989	24	3	277
1991	16	2	131
1992	83	5	303
1993	60	5	278
1994	74	4	308
1995	122	3	683
1996	136	7	579
1997	226	13	700

consistent with the positive centers of precipitation expansion coefficients of 20-year timescale in Figure 8a. In the last ten years, severe floods frequently happened along the Yangtze River in different reaches, such as in 1991 along the lower reach of the Yangtze River, 1998 and 1999 along the middle and lower reaches of the Yangtze River.

9. Circulation Change over East Asia

At the timescale of secular variation, different climatic anomalies and environmental disasters centered mainly in 1950s $\sim$ 1960s and 1980s $\sim$ 1990s. Particularly, many disasters appeared in northern China. Figures 12a,b show the mean summer (June–July–August) winds of 850 hPa averaged from 1955 to 1964 and from 1985 to 1994. Figures 13a,b show the mean winter (December–January–February) winds

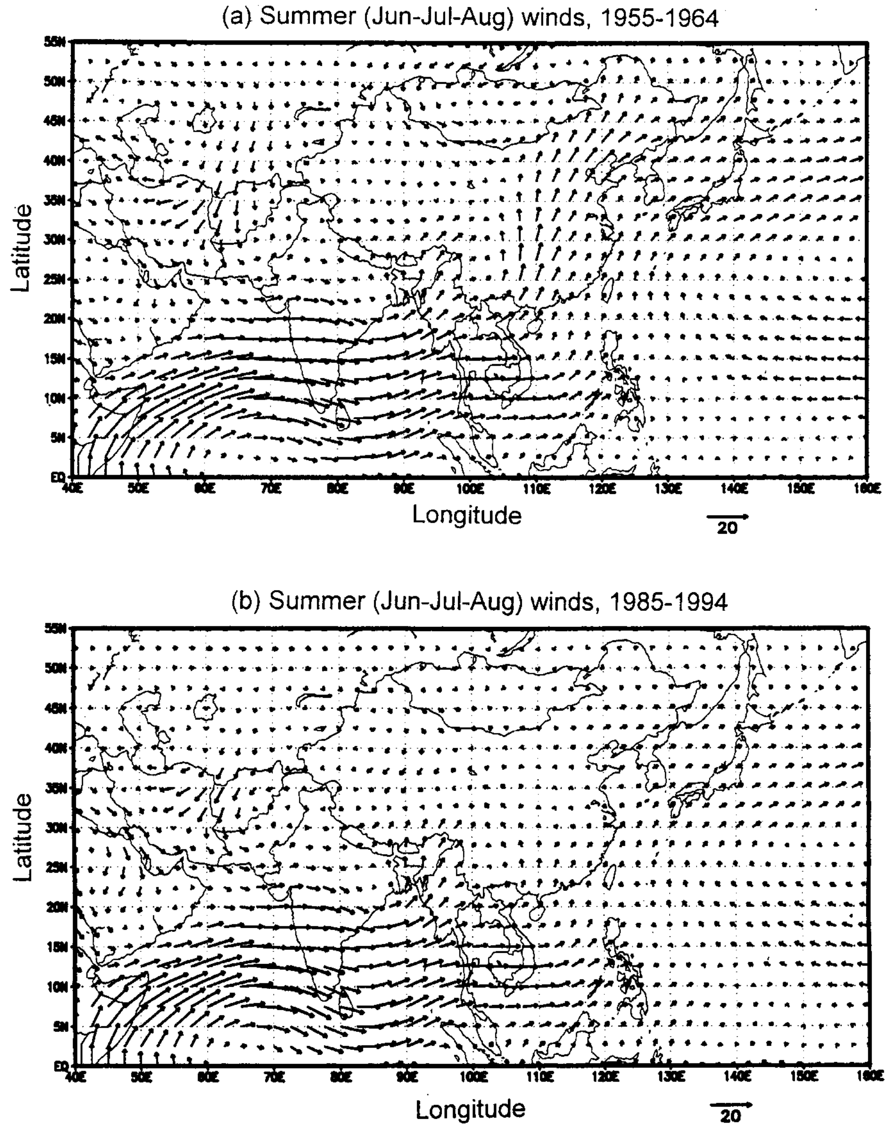

Figure 12. Mean summer (June–July–August) winds (m/s) of 850 hPa averaged (a) from 1955 to 1964 and (b) from 1985 to 1994.

of 850 hPa averaged from 1955 to 1964 and from 1985 to 1994. Different patterns of circulation can be found over eastern China in the above two periods. The strong southerly-southwesterly winds can reach North China, Northeast China, the Korean Peninsula and Japan for the summer of 1955–1964. Under the circulation pattern, the summer monsoon is strong and precipitation can be concentrated in northern China. As indicated by Figure 12b, very weak southerly winds appeared

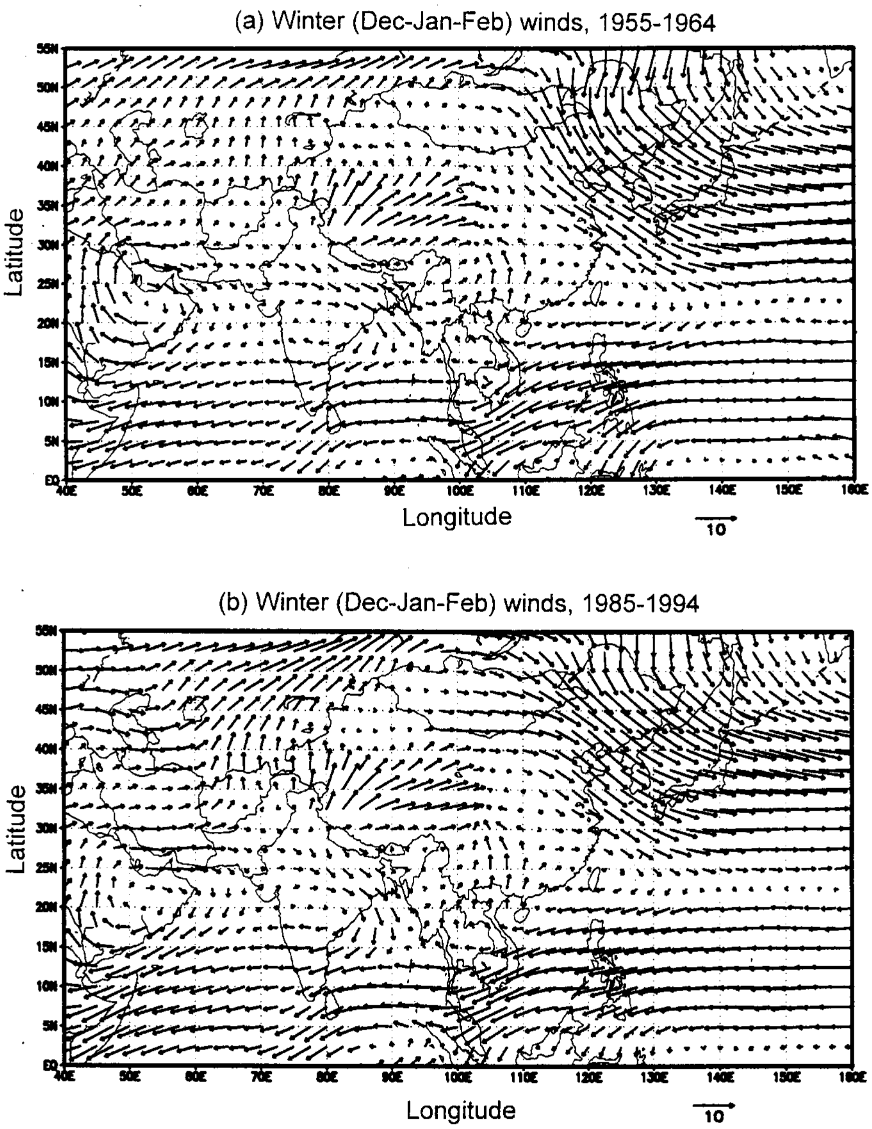

Figure 13. Mean winter (December–January–February) winds (m/s) of 850 hPa averaged (a) from 1955 to 1964 and (b) from 1985 to 1994.

in the summer of 1985–1994 over eastern China, but southwesterly winds can reach the lower Yangtze River. This pattern may explain why the summer floods could occur in southern China in the recent decade.

Comparing the patterns of winter circulation, it is noted that the northerly component of winds over northern China was stronger in 1955–1964 than that in 1985–1994. This strong northerly component may form stronger dry-cold winter climate in northern China. In East Asia, the phenomenon that the stronger summer monsoon will follow the stronger winter monsoon needs to be investigated for its reason. The temperature and precipitation changes shown in Figures 7 and 8 can be explained using these circulation patterns. Changes in interdecadal circulation may be the evolution indicator of the East Asian monsoon.

10. Concluding Remarks

In the last century, climate and environment experienced remarkable changes in different regions over China. Some interesting facts have been revealed through the present study. In Northeast China, the secular change of surface air temperature was found to be basically consistent with that in the Northern Hemisphere, and a positive contributor to global warming due to the larger amplitude was found. In the last two decades, temperature in the whole country has been rising continuously, but the largest range was found in Northeast China. More precipitation in the Northeast China appeared in 1940s ∼ 1950s while since 1970s precipitation has gradually decreased so that the dry trend has become more severe since 1970s in this region.

Despite the fact that there were differences between SATA in different reaches of the Yellow River valley or the Yangtze River valley, they have held the same secular change in the last century. The temperature was high from 1920s to 1940s while precipitation was below normal in the Yellow River valley from 1910s ∼ early 1940s, so drought mainly appeared over the period 1920s ∼ 1940s. Since the 1980s, less precipitation and higher temperature have happened again in the Yellow River valley, but the strength of drought is slightly weaker than that during the period of 1940s.

Along the Yangtze River valley, higher temperature appeared from 1920s to 1940s and has reappeared from 1990s. Less precipitation occurred in 1890s ∼ early 1900s and 1960s ∼ 1970s mainly, but more precipitation has appeared from late 1980s so that no dry trend has been noted in this region. At secular change, the climate in South China is moderate except for some smaller-scale variations.

Another fact is revealed that a quasi-20-year oscillation and a quasi-70-year oscillation obviously exist in temperature and precipitation series in different regions over China. The phase variations of SATA in Northeast China, the Yellow River and the Yangtze River valleys as well as South China were consistent with each other at the 20-year timescale. This phenomenon implies that at this timescale cold surge and warm wave can influence China simultaneously. For the warm wave, large amplitudes were found in 1940s and 1990s.

A question is why the surface air temperature in all regions decreased from a higher level to a lower one within one decade from late 1940s. Some other problems, such as why the temperature rising in northern China was earlier than that in southern China and what has caused temperature rising in all regions in the recent decade, need to be given more detailed study.

Drought trend and human activity in northern China have induced more severe environmental problems. Environmental change and human activity through the hydrological cycle has resulted in the runoff variations in Northwest China, no-flow in the lower reach of the Yellow River and the salinization of soil in Northeast China. On the other hand, frequent floods along the Yangtze River and high frequency of drought disaster have caused enormous losses during the last decade over China. Naturally, certain environmental change related to major variation of climatic parameter, or the relationship between them, such as the degree of drought disaster and drought index, the runoff (no-flow) or flood and atmospheric precipitation, and the dust storm and surface air temperature, have been analyzed. The primary reason for the trend of environmental changes may be linked with the evolution of the East Asian monsoon system in the last century.

Acknowledgements

The authors wish to thank Prof. S. W. Wang for providing data sets of surface air temperature anomalies and precipitation in China. The days of dust storms were obtained from Beijing weather station. We extend our thanks to the two anonymous reviewers for many helpful comments. This research was supported by the National Key Program for Developing Basic Sciences in China (No. G1999043405) and the National Natural Foundation of China (Contract No. 49975023).

References

Berger, W. H. and Labeyrie, L. D.: 1987, *Abrupt Climatic Change*, Reidel, Dordrecht, Boston, Lancaster, Tokyo, pp. 31–45.

Damage Report: 1995, *Report of the Damage Caused by Disaster in China*, China Statistical Press, Beijing, pp. 1–406.

Diaz, H. F.: 1986, 'An Analysis of Twentieth Century Climate Fluctuations in Northern North America', *J. Clim. Appl. Meteorol.* **25**, 1625–1657.

Diaz, H. F. and Quayle, R. G.: 1980, 'The Climate of the United States since 1895: Spatial and Temporal Changes', *Mon. Wea. Rev.* **108**, 149–226.

Fu, C. B., Diaz, H. F., Dong, D. F., and Fletcher, J. O.: 1999, 'Changes in Atmospheric Circulation over Northern Hemisphere Oceans Associated with the Rapid Warming of the 1920s', *Int. J. Clim.* **19**, 581–606.

Goudie, A. S. and Middleton, N. J.: 1999, 'The Changing Frequency of Dust Storms through Time', in Wilhite, D. A. (ed.), *Drought, Vol. II: A Global Assessment*, Routledge, London and New York, pp. 322–339.

Gruza, G., Rankova, E., Razuvaev, V., and Bulygina, O.: 1999, 'Indicators of Climate Change for the Russian Federation', *Clim. Change* **42**, 219–242.

IPCC: 1996, in Houghton, J. T., Meira Filho, L. G., Callander, B. A., Harris, N., Kattenberg, A., and Maskell, K. (eds.), *Climate Change 1995. Summary for Policymakers*, Cambridge University Press, Cambridge, pp. 1–7.

Jiang, J., Zhang, D., and Fraedrich, K.: 1997, 'Historical Climate Variability of Wetness in East China (960–1992): A Wavelet Analysis', *Int. J. Clim.* **17**, 968–981.

Jones, P. D., Wigley, T. M. L., and Wright, P. B.: 1986a, 'Global Temperature Variations between 1861 and 1984', *Nature* **322**, 430–434.

Jones, P. D., Raper, S. C. B., Bradley, R. S., Diaz, H. F., Kelly, P. M., and Wigley, T. M. L.: 1986b, 'Northern Hemisphere Surface Air Temperature Variations: 1850–1984', *J. Clim. Appl. Meteorol.* **25**, 161–179.

Karl, T. R., Knight, R. W., and Plummer, N.: 1995, 'Trends in the High-Frequency Climate Variability in the Twentieth Century', *Nature* **377**, 217–220.

Lau, K-M. and Weng, H-Y.: 1995, 'Climate Signal Detection Using Wavelet Transform: How to Make a Time Series Sing', *Bull. Amer. Meteorol. Soc.* **76**, 2391–2402.

Miller, A. J., Cayan, D. R., Barnett, T. P., Graham, N. E., and Oberhuber, J. M.: 1994, 'The 1976–1977 Climate Shift of the Pacific Ocean', *Oceanography* **7**, 21–26.

Pedj, D. A.: 1975, 'On the Indicator of Drought and Moisture Surplus', in *Proceedings of HMC of USSR* **156**, pp. 19–38 (in Russian).

Trenberth, K. E.: 1990, 'Recent Observed Interdecadal Climate Changes in the Northern Hemisphere', *Bull. Amer. Meteorol. Soc.* **71**, 988–993.

Wang, G., Shi, F., Zheng, X., Gao, Z., Yi, Y., Ma, G., and Mu, P.: 1999, 'Natural Annual Runoff Estimation from 1470 to 1918 for Sanmenxia Gauge Station of Yellow River', *Adv. Water Sci.* **10**, 171–196 (in Chinese with English abstract).

Wang, S. W. and Zhao, Z. C.: 1987, *Foundation of Long-Range Weather Forecasting*, Shanghai Science and Technology Press, Shanghai, pp. 1–201.

Wang, S. W., Ye, J. L., Gong, D. Y., and Zhu, J. H.: 1998, 'Construction of Mean Annual Temperature Series for the Last One Hundred Years in China', *Quart. J. Appl. Meteorol.* **9**, 392–401 (in Chinese with English abstract).

Yamamoto, R., Lwashima, T., and Sanga, N. K.: 1986, 'An Analysis of Climatic Jum', *J. Meteorol. Soc. Jpn.* **64**, 273–281.

Yan, Z. W.: 1999, 'Interdecadal Oscillations of Precipitation in North China and its Relation with Global Temperature Change', *Quart. J. Appl. Meteorol.* **10**, 16–22 (in Chinese with English abstract).

Yao, T. D., Jiao, K. Q., and Tian, L.: 1995, 'Climatic and Environmental Records in Guliya Ice Cap', *Sci. China* **38**, 228–237.

Yao, W., Zhao, Y., Tang, L., and Li, S.: 1999, 'Preliminary Study on No-Flow Disaster in the Lower Reaches of Yellow River', *Adv. Water Sci.* **10**, 160–164 (in Chinese with English abstract).

Ye, J. L., Chen, Z. H., Gong, D. Y., and Wang, S. W.: 1998, 'Characteristics of Seasonal Precipitation Anomalies in China for 1880–1996', *Quart. J. Appl. Meteorol.* **9**, 57–64 (in Chinese with English abstract).

Zhai, P. M., Sun, A. J., Ren, X. L., Gao, B., and Zhang, Q.: 1999, 'Changes of Climate Extremes in China', *Clim. Change* **42**, 203–218.

Zhang, D. E.: 1984, 'Climatic Analysis of the Dust Storm Weather in Chinese History', *Sci. China (B)* **3**, 278–288.

Zhang, H. L. (ed.): 1997, *Flood and Drought Disasters in China*, China Hydroelectric Press, Being, pp. 1–569.

(Received 4 February 2000; in revised form 29 March 2001)